

Hydrogen separation using electrochemical method

H.K. Lee^{a,*}, H.Y. Choi^b, K.H. Choi^c, J.H. Park^a, T.H. Lee^a

^a Department of Chemical Engineering, Yonsei University, 134 Shinchon-Dong, Seodaemun-Ku, Seoul 120-749, South Korea

^b LG Chem, Ltd., Seoul, South Korea

^c Samsung Advanced Institute of Technology, Seoul, South Korea

Received 8 September 2003; accepted 30 December 2003

Abstract

Hydrogen is separated from a hydrogen/nitrogen/carbon dioxide mixture by an electrochemical separation method. By applying a direct current to a proton-conducting membrane, hydrogen can be electrochemically dissociated on the platinum catalyst of the anode, transported across the hydrated cation exchange membrane, and then recovered on the catalytic cathode. The operating principles and advantages of the electrochemical hydrogen separation method are described. The effects of temperature and pressure are examined and the optimum operating conditions are determined. Increase in cell temperature enhances the purity of hydrogen and the power efficiency. The pressure of the feeding gas increases both the performance and the amount of hydrogen product, but decreases the purity of the hydrogen because of the increasing permeation flux of impurities, i.e., nitrogen and carbon dioxide. High purity, (99.72%) hydrogen can be achieved from a low purity (30%) feed via a two-stage separation process at 700 mA cm⁻².

© 2004 Elsevier B.V. All rights reserved.

Keywords: Electrochemical separation; Hydrogen purity; Power efficiency; Gas permeation; Polymer electrolyte membrane fuel cell

1. Introduction

Stable operation of a polymer electrolyte membrane fuel cell (PEMFC) on a feed stream of reformat gas is essential in demonstrating the utilization of PEMFCs for power generation. In recent years, there have been numerous studies to lower the levels of impurities that can be present in hydrogen fuel for PEMFCs. For instance, a catalytic steam reformer for the oxidation of methanol has been used to generate a hydrogen-rich gas mixture that is suitable for the fuel cell anode. The reforming reaction does not, however, provide pure hydrogen; rather, it produces a mixture of gases, namely, H₂, CO₂, N₂ and CO. Although this mixture is hydrogen-rich, the other components can restrict the performance of the anode severely [4,5]. Thus, an efficient means for separating pure hydrogen from the other constituents and several studies have examined the membrane separation process [6].

Gas separation through membranes was commercialized after the introduction of the Prism process by Monsanto two decades ago [1–3]. Though originally intended for hydrogen recovery, this process is now being used for the removal of various other components, most notably carbon dioxide, from mixtures on an industrial scale. The separation of un-

charged species in a typical membrane process is driven by a chemical potential gradient, $\Delta\mu$, according to the equation:

$$\Delta\mu_i = \mu_i - \mu'_i = RT \ln \left(\frac{a_i}{a'_i} \right) \quad (1)$$

where a_i denotes the activity of species i in the contaminated phase; a'_i represents the activity of species i extracted phase. General membrane separation depends upon a pressure gradient to drive one component of the mixture. Pressure differences of several hundred pounds per square inch are typical for this separation. The process does not produce a high-purity product, nor does it remove one component with perfect selectivity [7]. One attempt to solve these problems, has been the electrolytic transport of hydrogen in the form of protons across a solid polymer electrolyte in an electrolysis cell [8,9]. By applying a direct current to a proton exchange membrane, hydrogen can be electrochemically transported across the membrane. In an electrochemical separation, an electrochemical potential difference, $\Delta\bar{\mu}$, can provide a driving force across the membrane:

$$\Delta\bar{\mu}_i = RT \ln \left(\frac{a_i}{a'_i} \right) + z_i F \Delta\Phi_i \quad (2)$$

where $\Delta\Phi$ represents the applied electric potential; z_i the charge on species i , F is the Faraday constant. The electrochemical membrane method requires only an external elec-

* Corresponding author. Tel.: +82-2-312-6507; fax: +82-2-312-6401.
E-mail address: lhk1919@yonsei.ac.kr (H.K. Lee).

tric potential and no pressure nor concentration gradient. Electrochemical membrane separation can produce selectivity and efficiency that are considerably superior to those achieved in chemical membrane separations. This is because the electric potential difference in the former method affects only the charged species.

Many studies [10–12] have demonstrated that, by improving the conductivity of electrolytes and designing devices for the separation, the removal or the supply of hydrogen from a hydrogen containing atmosphere can be achieved with a SrCeO₃-based proton conductive solid electrolyte. These high-temperature-type proton conductive ceramics are used as electrolytes in solid oxide fuel cells (SOFCs) and can be operated stably at 800–1000 °C.

In the present work, the separation of pure hydrogen from a hydrogen/nitrogen/carbon dioxide mixture by a low-temperature electrochemical separation system is investigated. The apparatus for separating hydrogen is similar to that used in a PEMFC for producing an electrical current. Therefore, the electrochemical parameters, i.e., activation loss, ohmic loss, and mass transport loss, are generally in accordance with those of a PEMFC. When the gas mixture is supplied to the anode side of an electrochemical cell using a proton exchange membrane and direct current is passed through it, hydrogen is ionized on the platinum catalyst sites in the porous, gas-diffusion electrode and the resulting H⁺ protons are selectively transported through the membrane to the cathode where hydrogen gas is evolved. Pure hydrogen gas can be separated without pressurization and the separation rate can be easily controlled by the applied current.

2. Experimental

2.1. Membrane and electrode assembly

Nafion 115 (0.127 mm in thickness; ion-exchange capacity 1.01–1.03 meq/g dry membrane) manufactured by Du Pont was used as an ion-exchange membrane. The membranes were cleaned by immersion in boiling 3% H₂O₂ for 1 h, and then in H₂SO₄ for 1 h, to remove any metallic impurities. The membrane was then rinsed in boiling de-ionized water for 1 h and the procedure was repeated at least twice to remove the sulfuric acid completely. The electrodes were supplied by E-TEK, and contained 0.4 mg Pt/cm². Prior to preparation of the membrane electrode assembly, the electrodes were impregnated with Nafion solution by a brushing technique and dried at 80 °C. After completing that treatment, the electrodes were assembled and hot-pressed in combination with the composite membrane at 120 °C and 3 t for 3 min.

2.2. Cell test

Hydrogen, nitrogen and carbon dioxide were combined in a gas mixer. The hydrogen composition was controlled

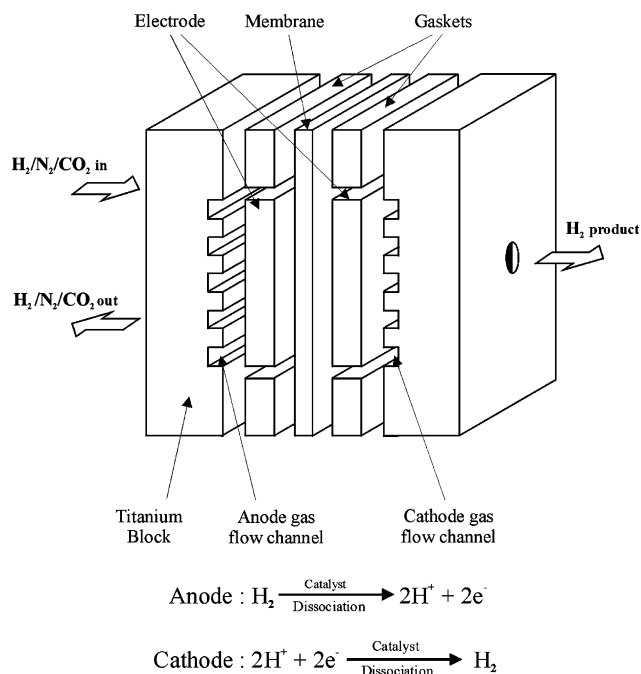


Fig. 1. Schematic diagram of single cell for gas separation.

from 10 to 90% and the ratio of nitrogen to carbon dioxide was 1:1. In order to maintain high ionic conductivity in the membrane, the gas mixtures were humidified before entering the cell by passing through a humidifier which was held at 10 °C above the cell temperature. The cell, shown in Fig. 1, was composed of titanium, two current-collectors and the membrane and electrode assembly. The surface area of the electrode was 5 cm².

The gas mixture was delivered to the fuel cell through a mass flow controller (Teledyne Hastings Raydist Co.). Direct current was supplied by a power supply (6410A, Hewlett Packard) and the separated gases were analyzed by gas chromatography (Hewlett Packard 5890II). Experiments were performed over a temperature range of 30–70 °C and over a feed pressure range of 1–3 atm.

2.3. Diffusivity measurement

The permeability and diffusivity of hydrogen and oxygen were determined by the time-lag technique [13–16]. This is a macroscopic technique that offers the advantage of a relatively simple experimental methodology and numerical interpretation. The process of permeation of gases through a dense polymer is classically described by the solution-diffusion model, that is, the gas is dissolved in water and it diffuses with water throughout the membrane. For this reason, measurements of gas permeability have to be carried out on fully-hydrated membranes.

A well-hydrated membrane with a cross-sectional area of 3 cm² was placed between the two O-rings of the cell. The latter was connected to a capillary tube in which water can move up when hydrated gas crosses the membrane. The dis-

placement of water was measured with respect to time and at a temperature of 70 °C. A steady state of gas permeation was approached after the decay of the transients. The cumulative amount, $Q(t)$, of gas that permeated through membrane in time t , was found to come close to the line expressed by:

$$Q = \frac{P_m \Delta P \times A}{L} \left(t - \frac{L^2}{6D} \right) \quad (3)$$

where P_m is the permeability coefficient; ΔP , the pressure difference across the membrane; A , the permeation area; L , the thickness of the membrane; D , the diffusion coefficient. The permeability value can then be obtained from the quasi steady-state part of the process, i.e., the slope of the straight line. The diffusion coefficient is easily calculated from the initial transitory regime, i.e., the intercept on the t -axis, which is called the time-lag (θ) and is given by:

$$\theta = \frac{L^2}{6D} \quad (4)$$

The solubility, S , is deduced using the relation: $P_m = D \times S$. The respective sorption and diffusion contributions can thus be split based on a single and rapid experiment.

3. Results and discussion

3.1. Hydrogen separation from $H_2/N_2/CO_2$ mixture

The voltage–current characteristics of electrochemical hydrogen separation at different cell temperatures and feed pressures are shown in Fig. 2. The relationship appears to be linear for the anodic and cathodic reactions of hydrogen in the solid polymer electrode. In theory, the line should ex-

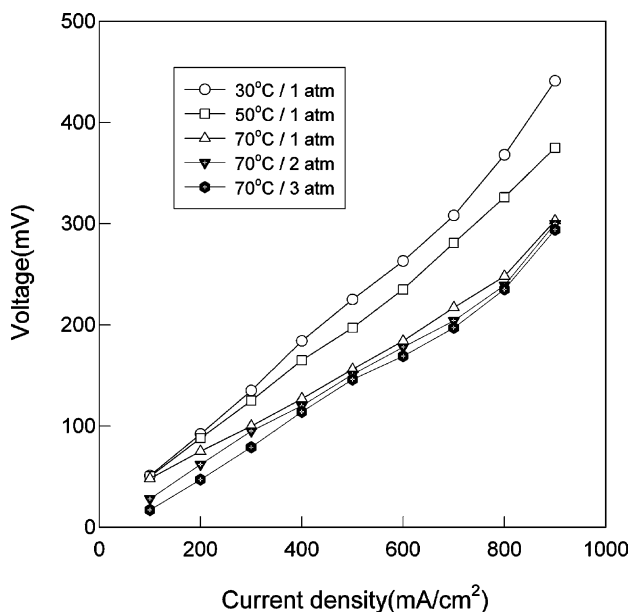


Fig. 2. Polarization characteristics for different cell temperatures and operating pressures (hydrogen inlet composition 50%).

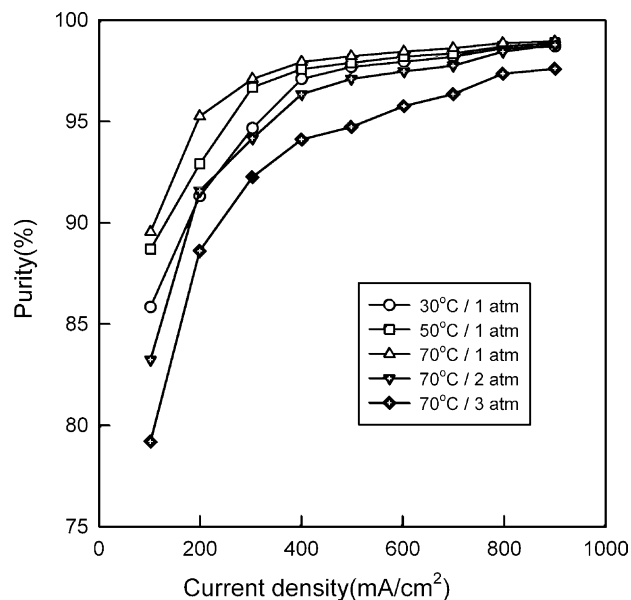


Fig. 3. Hydrogen purity vs. current density for different cell temperatures and operating pressures (hydrogen inlet composition 50%).

trapolate back to 0.000 V at zero current, but in the present experiments the hydrogen cathode is polarized by only a few millivolts due to a slight excess of protons near the anode [8].

The linearity of over potential characteristics suggests that, over the whole range of current density, the ohmic loss, i.e., electrolyte resistance expressed by $\eta_r = iR_r$, has more influence on the electrochemical hydrogen separation than mass transport loss. The latter results from the change in concentration of reactants at the surface of electrode. These observations indicate that minimization of the membrane resistance is an important factor in the efficacy of the electrochemical separation method.

In one set of experiments, the reaction temperature was varied from 30 to 70 °C while holding the cell pressure (1 atm) and the hydrogen inlet composition (50%) constant. The cell performance improved at elevated temperature since the reaction activity of the electrode and the conductivity of the membrane both increased.

In further experiments, the feed pressure was increased while the other parameters were kept constant. It was found that the performance was slightly improved as the pressure was increased, which was due to the increase in the partial pressure of hydrogen. This implies that the pressure gradient is not so effective in an electrochemical system as in a membrane separation system.

The relationship between hydrogen purity and current density is illustrated in Fig. 3. At the same temperature and pressure, hydrogen purity is enhanced with increased in current density because, according to Faraday's law, the proton flux through the membrane increased while the amounts of impurities, i.e., nitrogen and carbon dioxide, are not influenced by the current density and permeate across the mem-

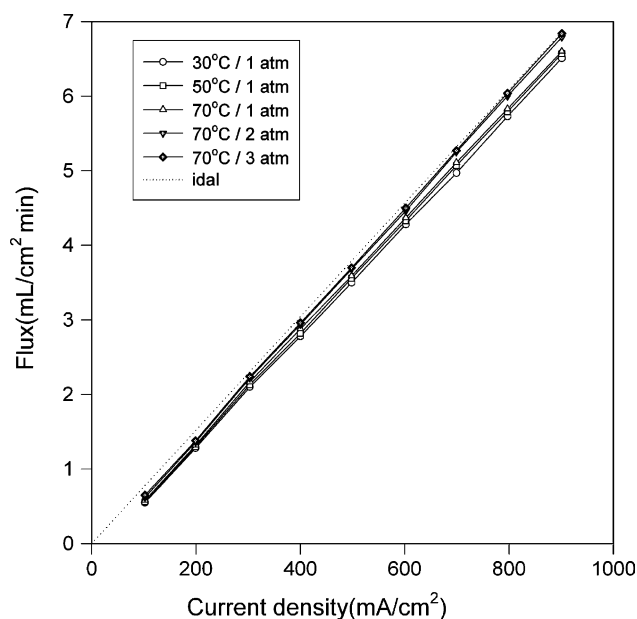


Fig. 4. Product flux vs. current density for different cell temperatures and operating pressures (hydrogen inlet composition 50%).

brane without being changed. The purity of hydrogen is also improved with increase in cell temperature due to increase in both the activity of hydrogen and the conductivity of the membrane. By contrast, a decrease in hydrogen purity is observed with increase in pressure. This can be explained by the fact that the amounts of nitrogen and carbon dioxide that permeate through the membrane under the influence of the pressure gradient are more than that of hydrogen. The permeation of impurity gases through membrane is proportional to the difference in partial pressure. The rate of hydrogen extraction from the gas mixture at 70 °C and 1 atm feed pressure is shown in Fig. 4. As mentioned above, the evolution rate obeys Faraday's law. Increases in cell temperature and feed pressure cause negligible growth of flux.

In electrochemical separation, the current efficiency is defined as the ratio of electrons used for generating hydrogen and computed as follows:

$$\varepsilon_i = \frac{\text{Real H}_2 \text{ product}}{\text{Theoretical H}_2 \text{ product}} \quad (5)$$

The theoretical hydrogen product is a function of current density only and is derived by assuming that the hydrogen is an ideal gas. At constant temperature and pressure, the current efficiency increases with current density. The current efficiency is also enhanced with cell temperature and operating pressure, because hydrogen dissociation, proton transfer reactivity in the Nafion membrane and the partial pressure of hydrogen all increase with temperature and pressure.

The voltage efficiency, ε_v , of hydrogen transfer can be computed relative to the thermal energy contained in the recovered hydrogen, i.e.,

$$\varepsilon_v = 1 - \frac{V}{1.484} \quad (6)$$

In this equation, 1.484 V is the voltage equivalent of the heat of combustion of hydrogen. The effect of temperature and pressure on the voltage efficiency is similar to the effect on polarization characteristics. The changes in voltage and current efficiencies with current density at different temperatures and pressures are shown in Tables 1 and 2.

The power efficiency is defined as $\varepsilon = \varepsilon_v \varepsilon_i$ and exhibits a maximum because ε_i increases and ε_v decreases with increasing current density. The results are given in Fig. 5. The power efficiency exhibits a maximum at about 300 mA cm⁻² and this current density is considered to be an optimum value with respect to power consumption.

3.2. Effect of hydrogen inlet composition

To investigate the influence of hydrogen feed composition on the cell characteristics and the purity of product hydrogen, the composition of the gases was varied from 10 to 90% while the other operating conditions (cell temperature: 70 °C; cell pressure: 1 atm) were constant. The results are given in Fig. 6. As the ratio of hydrogen to impurities decreases, the cell performance decreases. In other words, the partial pressure of hydrogen influences the electrochemical separation of hydrogen.

Table 1
Current efficiency and voltage efficiency as a function of current density at different temperatures

Current density (mA cm ⁻²)	Current efficiency (%)			Voltage efficiency (%)		
	30 °C	50 °C	70 °C	30 °C	50 °C	70 °C
100	70.87	72.16	74.74	96.56	96.63	96.77
200	84.54	85.87	87.19	93.80	94.07	94.95
300	91.10	92.40	94.13	90.90	91.58	93.26
400	91.35	92.66	94.64	87.60	88.88	91.44
500	92.38	93.96	94.75	84.84	86.73	89.49
600	93.45	94.54	95.41	82.28	84.16	87.60
700	93.46	95.34	96.09	79.25	81.06	85.38
800	94.50	95.49	96.15	75.20	78.03	83.29
900	94.97	95.84	96.28	70.28	74.73	81.60

Table 2
Current efficiency and voltage efficiency as a function of current density at different feed pressures

Current density (mA cm^{-2})	Current efficiency (%)			Voltage efficiency (%)		
	1 atm	2 atm	3 atm	1 atm	2 atm	3 atm
100	74.74	79.89	83.76	96.77	98.11	98.85
200	87.19	89.83	91.15	94.95	95.82	96.83
300	94.13	96.30	97.17	93.26	93.60	94.68
400	94.64	96.61	97.27	91.44	91.91	92.32
500	94.75	97.13	97.66	89.49	89.82	90.16
600	95.41	97.38	98.25	87.60	88.01	88.61
700	96.09	98.72	99.10	85.38	86.25	86.73
800	96.15	98.95	99.61	83.29	83.89	84.16
900	96.28	99.05	99.78	79.58	79.78	80.19

The overpotential characteristics of the inlet gases with compositions from 50 to 90% are linear over the whole range of current density. The resistance is predominantly due to the flow of protons through the membrane, i.e., electrolyte resistance. By contrast, the overpotential characteristics of 10 and 30% inlet compositions display a different tendency in the high current density region where a decrease in hydrogen mole fraction in the gas mixture has an effect on the concentration loss. Since nitrogen and carbon dioxide gases occupy a substantial portion of the reaction zone, the effective reaction area is reduced and the dispersion of hydrogen is hindered. This is related to the concentration loss, i.e., the mass transport loss, and can be expressed by the Nernst equation.

The purity of hydrogen as a function of current density, is shown in Fig. 7. The ratio of hydrogen to impurities has no effect on the purity of the hydrogen generated. This implies that high purity can be achieved from a hydrogen-containing

atmosphere by only a one-stage process without being affected by the inlet composition. The power efficiency is maximum at about 300 mA cm^{-2} and decreases by only 2–3% with decrease in the proportion of hydrogen in the hydrogen/nitrogen/carbon dioxide mixture.

3.3. Hydrogen separation by a two-stage process

Hydrogen was separated from a $\text{H}_2/\text{N}_2/\text{CO}_2$ mixture when the hydrogen inlet composition was 30%, through a two-stage separation process, i.e., two single cells were connected continuously. The ratio of nitrogen and carbon dioxide was 1:1, the cell temperature was 70°C and the feed pressure was 1 atm. The dependence of hydrogen purity on current density for the one-stage process is shown in Fig. 8. At 900 mA cm^{-2} , the purity is 98.92% at the first stage and 99.76% at the second stage. It should be noted that even at a low current density such as 100 mA cm^{-2} , the purity of hydrogen can be raised to 97.39%. The purity

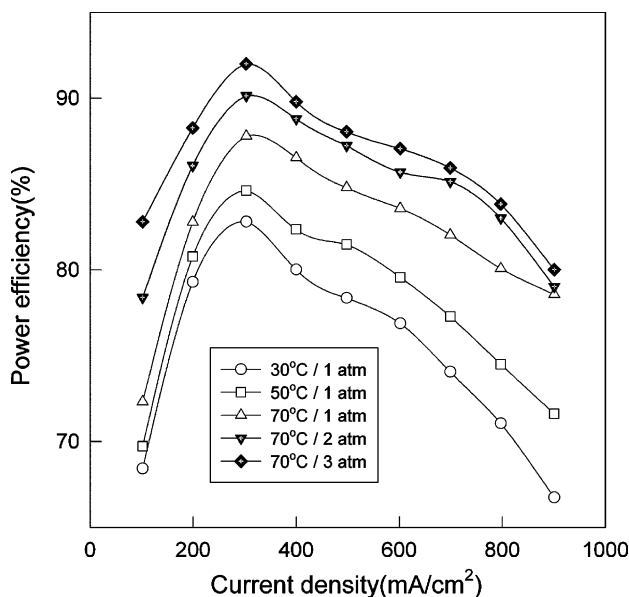


Fig. 5. Power efficiency vs. current density for different cell temperatures and operating pressures (hydrogen inlet composition 50%).

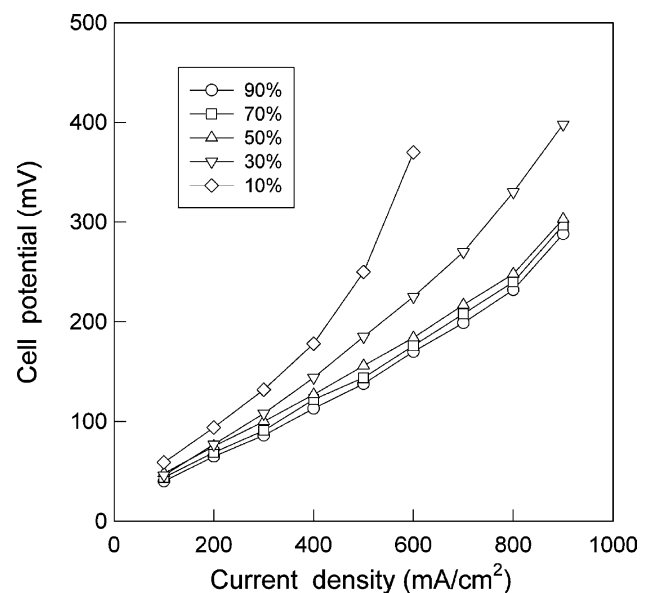


Fig. 6. Polarization characteristics for different hydrogen inlet compositions (7°C , 1 atm).

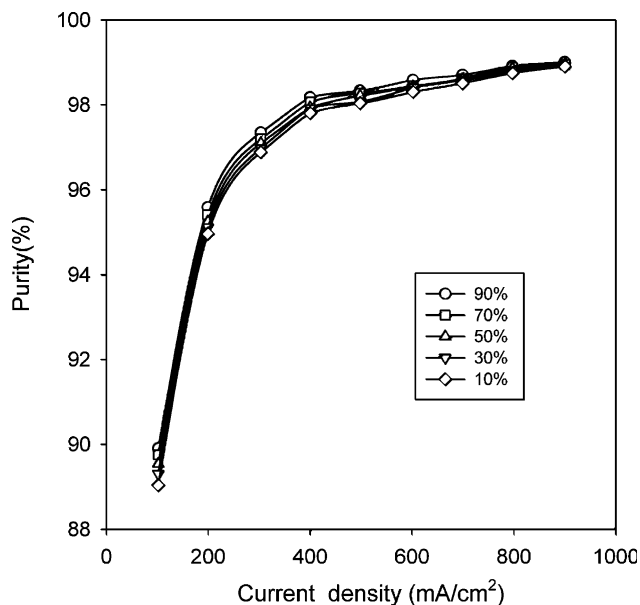


Fig. 7. Hydrogen purity vs. current density for different hydrogen inlet compositions (7 °C, 1 atm).

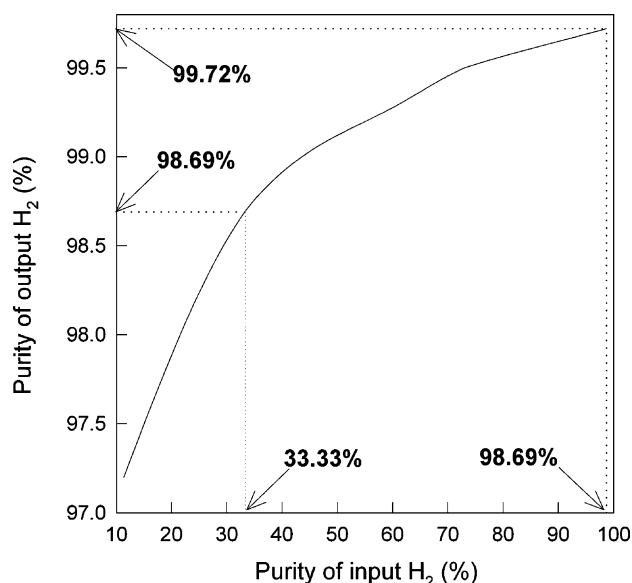


Fig. 9. Relation between purity of input gas and purity of output gas (7 °C, 1 atm, feed H₂ purity 30%, 700 mA cm⁻²).

of hydrogen can be predicted by the relation between the purity of input gas and that of output gas, as illustrated by Fig. 9. The purity of hydrogen can be predicted by selecting operating current density for a particular feed stream. At 700 mA cm⁻², 98.6 and 99.73% of hydrogen gas can be obtained from 33% inlet gas via a one-stage process and a two-stage separation process, respectively.

Permeation of nitrogen/carbon dioxide through the membrane is the major factor that degrades the purity of hydrogen. Without changing the current density, the volume of gas permeating the membrane was measured under the same

Table 3
Permeability, diffusion and solubility of gases (70 °C, 1 atm)

	P_m^a ($\times 10^9$)	D^b ($\times 10^8$)	S^c ($\times 10^2$)
N ₂	4.7	6.20	7.6
N ₂ + CO ₂	13	11.1	12
CO ₂	18	14.6	12

^a Permeability coefficient (cm³ cm/(cm² s cmHg)).

^b Diffusivity coefficient (cm² s⁻¹).

^c Solubility (cm³/cm³-cmHg).

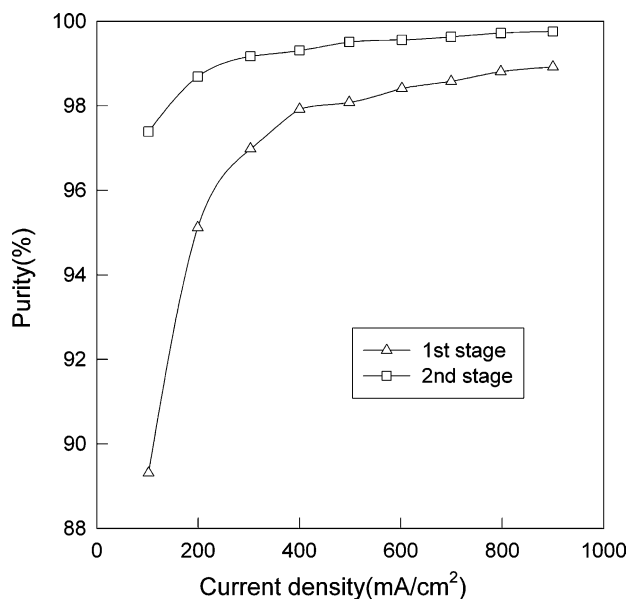


Fig. 8. Product purity vs. current density between first stage and second stage (7 °C, 1 atm, feed H₂ purity 30%).

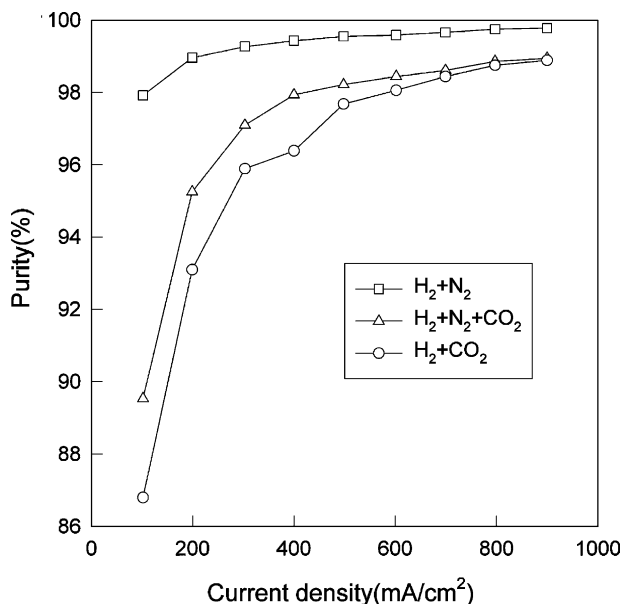


Fig. 10. Comparison of hydrogen purity for different mixed gases at 70 °C, 1 atm.

conditions of gas separation. Using time-lag method, the coefficient of permeation and diffusivity was calculated. After that, the solubility was obtained by the above mentioned relation $P_m = D \times S$. The results are summarized in Table 3. The permeation volume of carbon dioxide is greater than that of either nitrogen alone, or the nitrogen/carbon dioxide gas mixture. The permeability coefficient of carbon dioxide is $18 \times 10^{-9} \text{ cm}^3 \text{ cm/cm}^2 \text{ s cmHg}$ whereas the nitrogen was $4.7 \times 10^{-9} \text{ cm}^3 \text{ cm/cm}^2 \text{ s cmHg}$. The results from permeation experiments are similar to those of the electrochemical separation process, cf., Figs. 10 and 8.

4. Conclusions

Hydrogen has been separated from a hydrogen/nitrogen/carbon dioxide gas mixture by an electrochemical method that uses a proton exchange membrane. The separation characteristics, purity of the product hydrogen and power efficiency are obtained under different operating cell temperatures and feed pressures. The purity of hydrogen can be enhanced by a two-stage separation process, and the permeation of nitrogen and carbon dioxide has been evaluated. Cell characteristics, hydrogen purity, flux and efficiencies are all increased as the cell temperature is raised. An increase in feed pressure causes increases in flux and efficiencies, but lowers the hydrogen purity. In all cases, the power efficiency has a maximum value at 300 mA cm^{-2} . High purity, viz., 97.39%, can be achieved from a low purity feed, viz., 30%, through a two-stage separation process at 100 mA cm^{-2} . The permeability of carbon dioxide is larger than that of nitrogen, so the purity of hydrogen is influenced more by carbon dioxide than by nitrogen. These preliminary studies demonstrate that electrochemical separation is a feasible means for the recovery of hydrogen as a by-product from gas manufacturing processes and of-

fers advantages over the conventional route of membrane separation.

Acknowledgements

This work was supported by a Korea Research Foundation Grant. (KRF-2002-A1008-2002-005-E00030).

References

- [1] J. Winnick, Chem. Eng. Prog. 86 (1990) 41.
- [2] R.W. Rousseau, Handbook of Separation Process Technology, Wiley, New York, USA, 1987.
- [3] H. Gerischer, C.W. Tobias, Advances in Electrochemical Science and Engineering, VCH, 1990.
- [4] G.J.K. Acres, J.C. Frost, G.A. Hards, R.J. Potter, T.R. Ralph, D. Thompsett, G.T. Burstein, G.J. Hutchings, Catal. Today 38 (1997) 393.
- [5] C. Sishla, G. Koncar, R. Platon, S. Gamburgzev, A.J. Appleby, J. Power Sources 71 (1998) 249.
- [6] K.E. Cox, in: Proceedings of the 2nd World Hydr. Eng. Conference, Zurich, Switzerland, 1978, pp. 21–24.
- [7] J. Johnson, J. Winnick, Sep. Purif. Technol. 15 (1999) 223.
- [8] J.M. Sedlak, J.F. Austin, A.B. La Conti, Int. J. Hydrogen Energy 6 (1981) 45.
- [9] J.J. Zupancic, U.S. Patent, 4,664,761 (1987).
- [10] H. Iwahara, H. Uchida, N. Maeda, Solid State Ionics 11 (1983) 109.
- [11] H. Iwahara, H. Matsumoto, K. Takeuchi, Solid State Ionics 136 (2000) 133.
- [12] W. Münch, K.-D. Kreuer, G. Seifert, J. Maier, Solid State Ionics 136 (2000) 183.
- [13] G.E. Zaikov, A.L. Iordanskii, V.S. Markin, Diffusion of Electrolytes in Polymers, Institute of Chemical Physics, Moscow, USSR.
- [14] J.G.A. Bitter, Transport Mechanism in Membrane Separation Process, University of Twente Enschede, The Netherlands.
- [15] J. Sanchez, C.L. Gîjju, V. Hynek, O. Muntean, A. Julbe, Sep. Purif. Technol. 25 (2001) 467.
- [16] E. Favre, N. Morliere, D. Roizard, J. Membrane Science 207 (2002) 59.